Remote Sensing Applications: Fog Fluctuations, Vegetation Health, and Coastal Forest Fires in Northern California

Mina K. Burns

ABSTRACT

Coast redwood ecosystems along the northern California coastline are heavily reliant on fog and low cloud cover (FLCC) inputs, especially during dry summer months with lower precipitation. These ecosystems are also among the most vulnerable to irreversible damage from high severity wildfires. This study uses remote sensing imagery, primarily MODIS satellite data, to examine how variations in FLCC across different times and study areas impact the health of vegetation, indicated by the Normalized Difference Vegetation Index (NDVI). A Generalized Additive Model (GAM) was used to determine how FLCC fluctuations, along with climatic variables associated with fire, influence the severity of wildfires. Overall, FLCC days per month did not have a notable increase or decrease over the course of the study period, from 2000 to 2022. Additionally, fluctuations in FLCC are closely linked to variations in NDVI, with notable exceptions during drought periods. The results showed that precipitation, maximum vapor pressure deficit (VPD), and the Enhanced Vegetative Index (EVI) were significant in predicting the difference Normalized Burn Ratio (dNBR), but mean temperature and FLCC proportion were not significant in prediction power. Examining pre-ignition conditions revealed notably low FLCC and precipitation levels at each site, along with elevated maximum VPD and temperature. Results reveal the importance of fog in affecting vegetation health, along with the capabilities of using remote sensing technologies to monitor coastal forest ecosystems. Additionally, findings show that implementing forest management strategies during heightened risk for fire ignition events is crucial in addressing unprecedented high severity wildfires.

KEYWORDS

Vegetation health, fog and low cloud cover (FLCC), remote sensing tools, wildfire burn severity

INTRODUCTION

Coastal forests in northern California contain some of the oldest and most diverse biomes, including coast redwood ecosystems, which are also among the most susceptible to severe ecological damage from high severity wildfires (Mahdizadeh 2021, Potter 2023). Forest managers and researchers are interested in understanding the implications of recent wildfires occurrences and how they can effectively manage for future events. Although the full extent of climate change effects on fire behavior across the globe is not fully quantified, a new pattern of unprecedented high severity wildfires at a higher frequency throughout California has been associated with climate change (Westerling 2006, Miller 2009, van Mantgem 2013). Since 1984, high-severity wildfires in northern coastal California have been increasing by around 10% per decade (Huang 2020). Wildfires in this area have been immense in recent years, capturing the attention of resource managers, fire scientists, and the general public (Halofsky 2020). There are many shifting factors impacting wildfire, and one of the most elusive is the influence of fog in the region.

Changes in fog and low cloud cover (FLCC) frequency and associated climate variables have important implications for both vegetation of the region and wildfire occurrence. Cold upwelled ocean water along the coast is associated with strong warm-season subsidence, along with surface winds which create conditions for marine fog formation (Filonczuk 1995, Koračin 2014). Water from fog often makes up a significant proportion of hydrological factors of ecosystems, especially the coastal coniferous forests of northern California (Corbin 2005, Weathers 2020). These forests experience a significant reliance on fog as a water source, most notably during summer when rainfall is absent (Dawson 1998, Torregrosa 2016). Notable species such as coast redwood, or *Sequoia sempervirens*, have a limited range not more than 80 km inland of the coast (Johnstone 2010). *S. sempervirens* requires a high ratio of water supply to water loss, so without the consistent occurrence of summer fog, no true redwood forest is possible (Cooper 1917).

One way to quantify the relationship between fog and vegetation is using remote sensing data. Satellite observations are useful detectors of fog since they are able to differentiate between fog and other clouds or land surfaces based on infrared radiance properties (Gultepe 2009, Torregrossa 2014). Remotely sensed data makes the investigation of FLCC variability possible at a larger scale where ground proofing is not possible (Cermak 2018). Daily overpass imagery from satellites, such as the Moderate Resolution Imaging Spectroradiometer (MODIS), allows data users to determine FLCC presence at a highly detailed spatial and temporal resolution (Jensen 2008).

The utilization of remote sensing tools also facilitates the understanding of wildfire patterns and vegetation health by recording highly accurate records on wildfires in geospatial form and presenting metrics of vegetation productivity. One metric is the Normalized Difference Vegetation Index (NDVI), derived from NOAA's Advanced Very High Resolution Radiometer (AVHRR) instrument, which is an indicator of vegetation greenness and health (Pettorelli 2005, Eastman 2013). Remote sensing data and technologies have also been widely used for mapping and monitoring areas affected by fires (Matci 2020). One important climatic variable that is related to FLCC and burn severity is vapor pressure deficit (VPD). VPD is the difference between the actual water vapor content of the air and its saturation potential value, serving as a metric of the atmosphere's ability to extract moisture from land surface (Erard 2016). The measure of VPD is closely related to variability in burned forest areas in the western United States (Seager 2015). High VPD values lead to rapid water loss from plants, and if sustained, significantly dry out vegetative material (Williams 2014). Considering both VPD and FLCC is important to strengthen the burn severity model and determine the correlation strength of each climatic variable. Other studies have drawn conclusions between VPD and burn severity (Sedano 2014, Grünig 2023, Wasserman 2023), created FLCC or NDVI time series (Fensholt 2012, Nghiem 2019, Werner 2022, Eisfelder 2023), but none have done all of these while also incorporating FLCC into burn severity regression models.

This study utilizes current remote sensing tools and climatic variable datasets to determine the effects of FLCC level variability over time and across different regions on vegetation health, along with the increasing prevalence and severity of wildland coastal fires. The first subquestion examines the relationship between fog levels and vegetation growth along the northern California coast. I expected that coastal areas with high fog presence year-round (northern and coastal regions) will experience associated higher NDVI values than areas with low fog presence (southern and inland regions). The second subquestion explores the relationship between FLCC occurrence and other relevant climatic variables during the fire season and the occurrence and severity of burned area. I inferred that fog occurrence during the fire season will be a significant predictor of the difference Normalized Burn Ratio (dNBR) when used in a model with these other variables. The third subquestion asks what the overall fog patterns in the study region are when looking at the entire study period. I hypothesized that fog patterns in the northern California coastal forest study region will fluctuate, but during the 22-year study period, will show a decrease in fog days per month over time.

METHODS

2. Study Site

My study focuses on northern California coastal forests, which are generally defined as forests within 50 km of the coast (Noss 2013). Depending on the local topography, the true range of this ecosystem may be even more limited in extent from the coast, as fog may not penetrate as far inland (Torregrosa 2016). Coastal forests are among the most heavily affected by marine fog variation (Petreshen 2021).

In examining the relationship between fog levels and vegetation growth through the measurement of NDVI, I limited my focus to six locations in which wildfires occurred during the study period, from 2000 to 2022 (Figure 1). The correlation between fog occurrence and the severity of fire will also be determined by examining these six fire locations. These fires are located in the following areas: Sonoma County, Point Reyes, Santa Cruz and San Mateo counties, Klamath National Forest, and Napa and Lake counties (Table 1). Other fire events in northern California during recent years were either not large enough in extent and severity for the study purposes or did not meet the 50 km coastal proximity requirement.

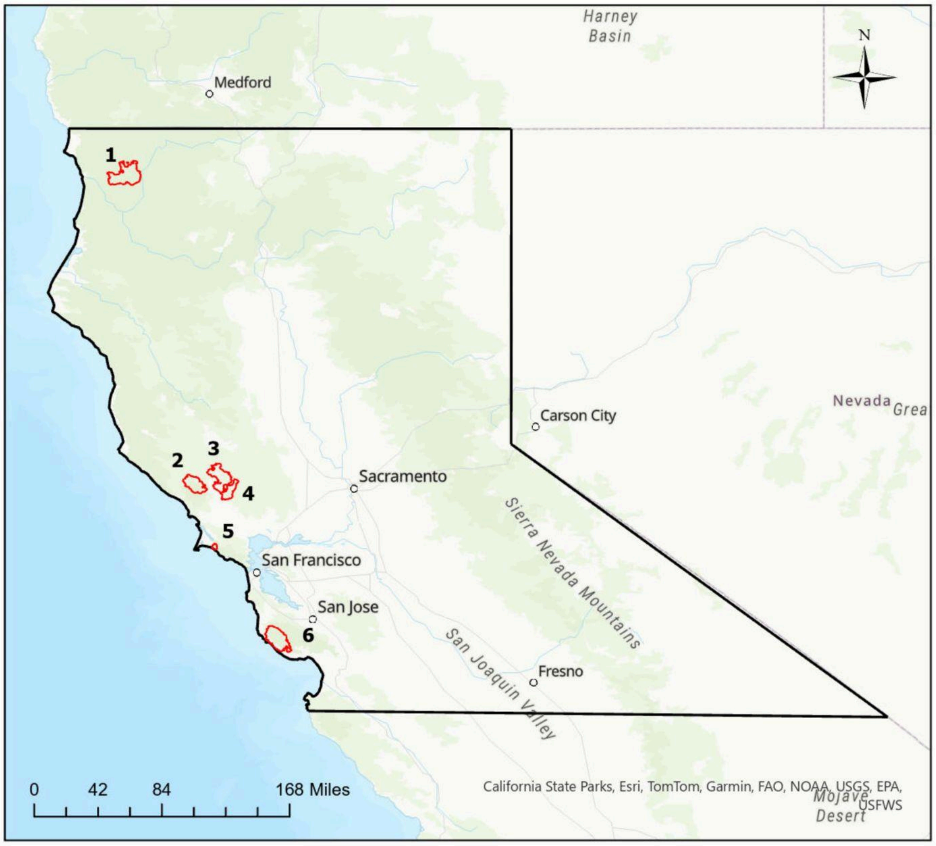

Figure 1. ArcGIS Pro map with the six study sites delineated. The Northern California boundary line is also defined (Burns 2024).

Table 1. Fires used in the study. Parameters include fire name, start and end date, fire location, fire size, elevation, and land cover type.

n	Fire Name	Start Date	End Date	Fire Location	Fire size (ha)	Elevation (m)	Vegetation / Landcover Type
1	Siskiyou	6-21-2008	9-30-2008	Klamath National Forest	77,715	465	coast redwood, conifer, grassland, hardwood
2	Walbridge	8-17-2020	10-2-2020	Sonoma County	22,260	465	coast redwood, conifer, grassland, hardwood
3	Kincade	10-23-2019	11-06-2019	Sonoma County	77,700	117	shrubland, mixed conifer-hardwood, grassland, vineyard
4	Tubbs	10-8-2017	10-31-2017	Lake/Napa/Sonoma counties	36,800	262	shrubland, hardwood, conifer, urban
5	Woodward	8-17-2020	10-1-2020	Point Reyes	2,020	180	conifer, wetland, shrub
6	CZU August Lightning Complex	10-16-2020	9-22-2020	Santa Cruz/San Mateo counties	86,000	400	grassland, coastal scrub, riparian woodland, coast redwood

I chose study sites both close to the Oregon-California border and south of the San Francisco Bay to examine the difference between latitudinal-based fog fluctuations, as northernmost coastal areas historically experience more fog days and greater productivity (Chen 2021). I also chose areas that are directly on the coast (e.g., Point Reyes, Santa Cruz), along with areas that are in the eastern extent of the coast redwood range (e.g., Sonoma County, Napa and Lake counties) (Figure 2). The eastern extent has a more sparsely populated redwood population instead of continuous redwood forest, and acts as an indicator of the border of shifting climatic conditions (Fernández 2015).

Figure 2. Coast Redwoods Distribution map. In California, from the CA Department of Parks and Recreation. February 2021.

2.1 Data Collection

My primary fog dataset was extracted from the MODIS 1km FLCC Google Earth Engine Application (Werner 2022). Moderate Resolution Spectroradiometer (MODIS) sensor data is largely available on a daily basis. The Terra MODIS satellite was used by Werner's team to create an FLCC dataset that spans over 20 years, from 2000-2022. The Terra MODIS cloud flags were evaluated to create a FLCC dataset along the California and southern Oregon coast for the summer months, June through September. The dataset was provided in a monthly summary as the number of fog days per month. In addition, the study author provided me with daily FLCC rasters of my study area, clipped to northern California, from June through September of 2020 (Z. Werner, *personal communication*). This data indicated fog presence through a binary system, 1 meaning FLCC presence and 0 meaning no FLCC presence as detected by MODIS.

To obtain burn severity shapefiles, I used the USDA Rapid Assessment of Vegetation after Wildfire (RAVG) Burn Severity Viewer (USGS 2022). This dataset uses satellite data to estimate post-fire vegetation conditions on National Forest System (NFS) lands, including the composite burn index (CBI), percent basal area loss, and percent canopy cover loss. To access the data for my study sites, I changed the date range to "2000-2022", and filtered by products RAVG, MTBS (Monitoring Trends in Burn Severity), and BAER (Burned Area Emergency Response). I downloaded the KMZ Wildfire Shapefiles, which were used to delineate each site.

The difference Normalized Burn Ratio (dNBR) is often used to assess fire severity, and is created by subtracting post-fire NBR from pre-fire NBR (Delcourt 2021) (Table 2). To obtain dNBR data, I accessed the Climate Engine database, which is a free web application that uses GEE to download and process a wide variety of climate and remote sensing datasets (Huntington 2017). I clipped to my specific fire boundaries and downloaded Earth Observations data at the daily scale, which I then summarized to a monthly value.

To access vegetative health data in the form of NDVI, I used the MODIS Terra Daily NDVI Data from the Google Earth Engine (GEE) Catalog. The Normalized Difference Vegetation Index (NDVI) is generated from the Near-IR and Red bands of each scene as (NIR - Red) / (NIR + Red), and ranges in value from -1.0 to 1.0 (Table 2). This product is generated from the "MODIS/MCD43A4_006_NDVI" surface reflectance composites (Gorelick 2016).

For relevant climatic variable data, I accessed the Parameter-elevation Regressions on Independent Slopes Model (PRISM) Climate Dataset, which gathers climate observations from a wide range of monitoring networks and develops spatial climate datasets to reveal climate patterns (Oregon State 2023). I downloaded .csv files for each study site for mean temperature, precipitation, and maximum vapor pressure deficit variables. Most of my analysis is done using the R package, 'prism', which allows users to access the Oregon State PRISM climate data and process the results.

Table 2. Spectral Indices. Includes Formula Description. NIR is the Near Infrared wavelength band, and SWIR is the short-wave infrared band.

n	Spectral Indices	Formula Description
1	Normalized Burn Ratio (NBR)	$NBR = \frac{NIR-SWIR}{NIR+SWIR}$
2	Difference Normalized Burn Ratio (dNBR)	$dNBR = [NBR_{\text{pre-fire}} - NBR_{\text{post-fire}}]$
3	Normalized Difference Vegetation Index (NDVI)	$NDVI = \frac{NIR-Red}{NIR+Red}$

2.2 Data Analysis

2.2.1 Fog and Vegetation

2.2.1.1 Google Earth Engine NDVI

Using the GEE Code Editor, I imported the shapefiles from RAVG for each of the six study sites and clipped my analysis to each area. I used the MODIS NDVI image collection to access the data, and filtered for my study dates: January 1, 2000, to December 31, 2022. Additionally, I also isolated dates with sensor information gaps and removed these points from the dataset to avoid generating faulty NDVI composite data. For each site, I downloaded the data into R Studio and generated a chart of long term time series after filtering NDVI for the summer months only. I added a marker to indicate the time of fire ignition events for each site. Creating a time series of NDVI allows for direct comparison with the FLCC time series for the same locations.

2.2.1.2 FLCC and NDVI Time Series

I downloaded rasters from the MODIS 1 km Monthly Fog and Low Cloud Cover 2000-2022 dataset. For each study site, I created a for loop in R Studio to extract the FLCC data for a specified coordinate. Then, I divided the number of fog days by the numbers of days in each month to create an FLCC proportion variable. To determine the relationship between NDVI and FLCC proportion, I plotted the two variables on the same chart for the same time period for each site, after standardizing the variables for direct comparison. For each study site, plotting monthly NDVI and FLCC proportion as a correlation plot did not yield a significant linear relationship, so I found it more fitting to examine the variables in a time series setting.

2.2.2 Fog and Burn Severity

2.2.2.1 Generalized Additive Model

To determine the relationship between burn severity and FLCC, I used a Generalized Additive Model (GAM) (Formula 1). The GAM is an additive modeling technique that does not make assumptions about the underlying distribution of the dataset, along with using smooth functions to capture the impact of predictive variables (Stasinopoulos 2024). My initial methodology, the multivariate linear regression (MLR) model, did not lead to conclusive results due to the non-linear relationships of the variables, so the GAM was better suited to the data.

The GAM model used five inputs to predict dNBR, with data from each study site (Figure 3). I used the Climate Engine dNBR data, FLCC proportion data, along with additional variables from PRISM that are known to affect burn severity: precipitation, maximum VPD, and mean temperature (Dillon 2011, Abatzoglou 2013). I also used the Enhanced Vegetation Index (EVI) from Climate Engine, which is a vegetation metric similar to NDVI but different in that it uses a blue band in addition to the red and NIR bands (Jiang 2008). After downloading the data and preprocessing it in R Studio, I used the 'gam' function from the mgcv package (Wood 2017). Generating a summary of the model outputs the parametric coefficients, significance of each smooth term, adjusted R-squared, and deviance explained by the model.

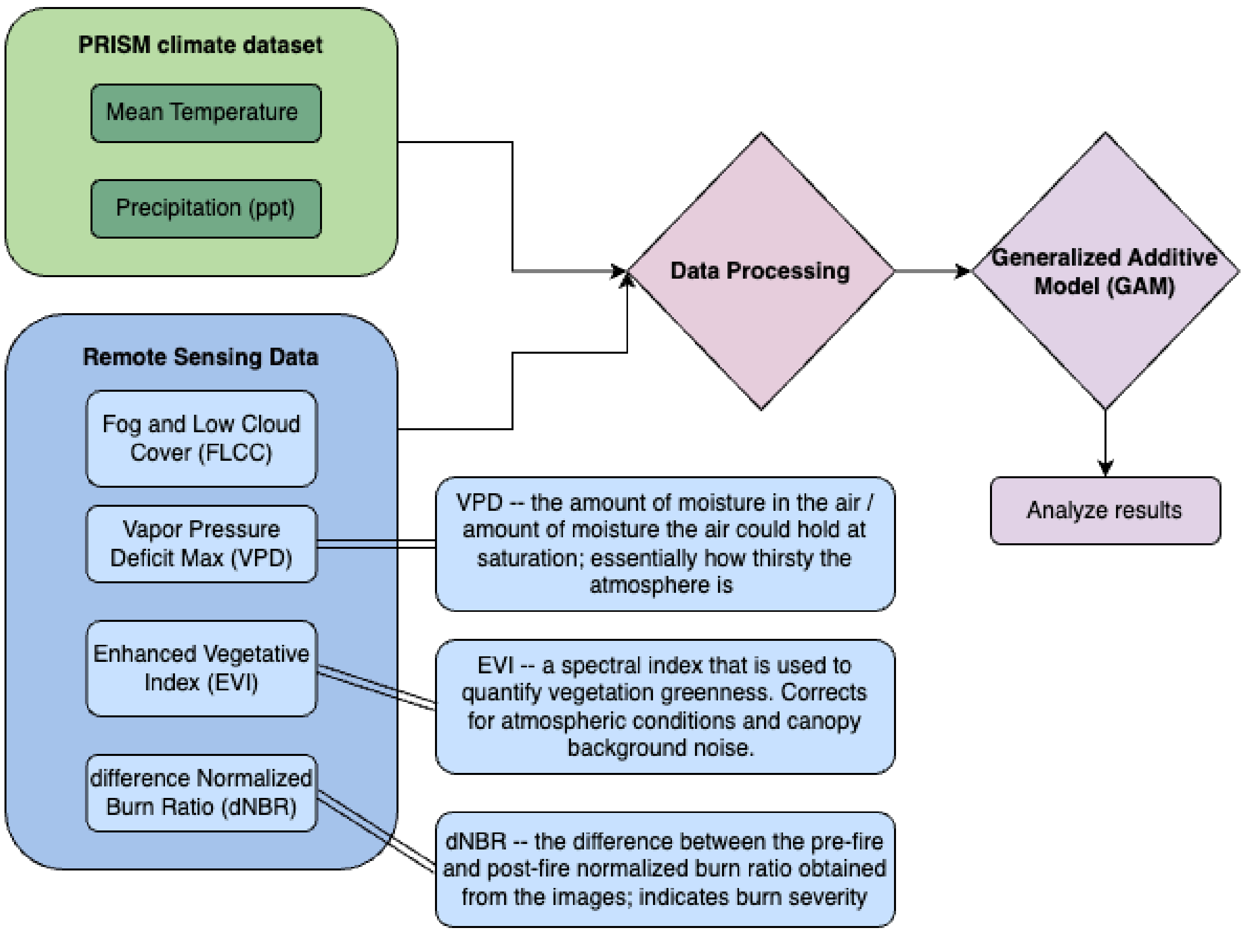

Figure 3. Burn Severity Model Flowchart. Relevant climatic variables are included and defined.

Formula 1. Generalized Additive Model. The model relates a univariate response variable, Y, to some predictor variables, s_i.

$$g(E(Y)) = \alpha + s_1(x_1) + \cdots + s_p(x_p)$$

2.2.3 Fog Trends

2.2.3.1 FLCC Time Series

Using the generated fog proportion from the MODIS 1 km FLCC dataset, I carried out a time series analysis of FLCC cover for each of the six study sites. I used the entire period of data available, from 2000 to 2022 for summer months, to create a smoothed trendline for the data, with +/- 1 standard error (Figure 4).

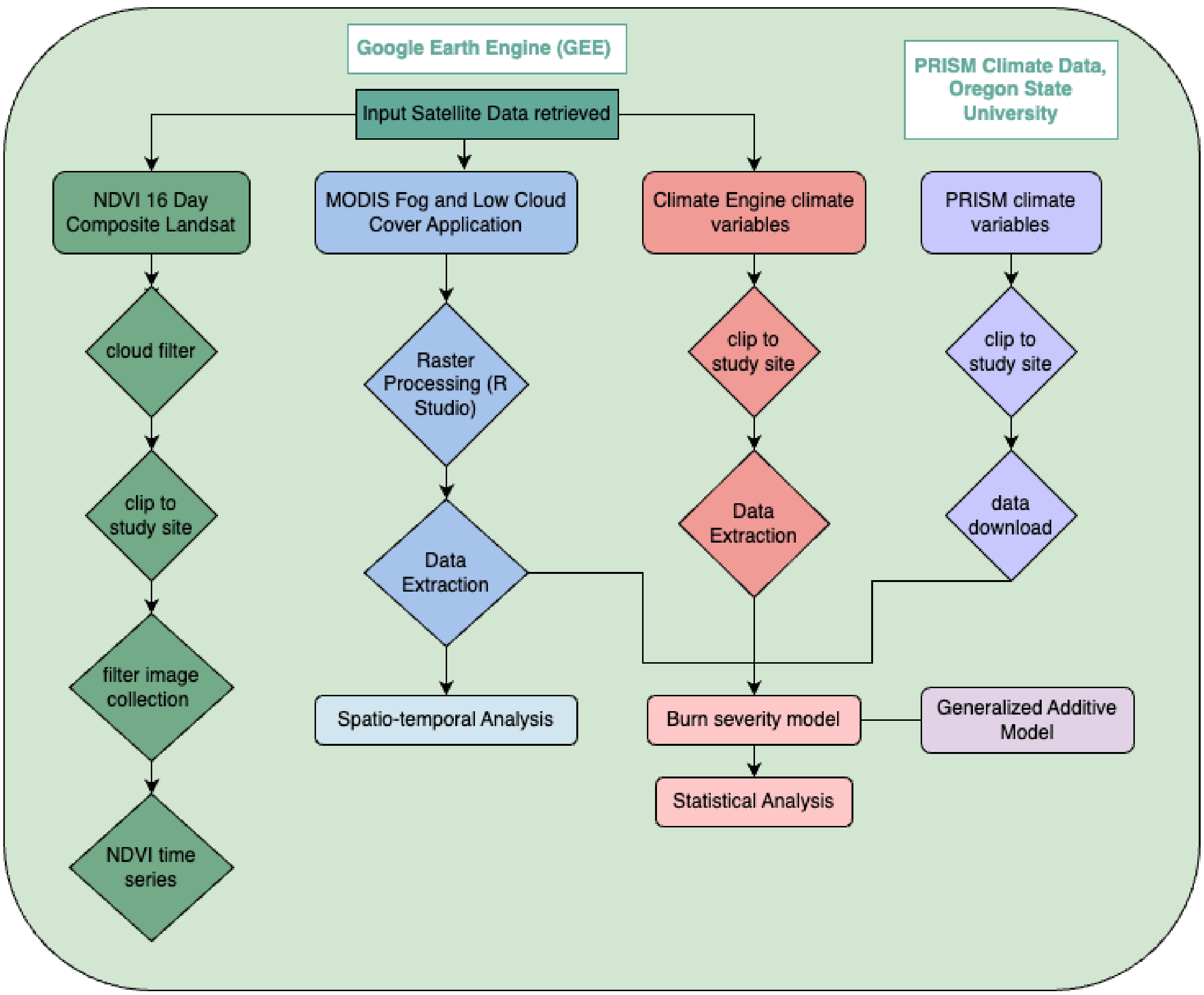

Figure 4. Methods flowchart and data sources. A summary of the entire methodology, including data sources.

2.2.4 Pre-ignition conditions

To examine ignition conditions at each study site, I isolated FLCC proportion, precipitation, maximum VPD, and mean temperature and looked at the variables at each fire start date, for the period leading up to the fire and at the time of ignition.

Results

Google Earth Engine NDVI

While the average monthly NDVI had a seasonal fluctuation at each study site, I found that it was highest at the Woodward and CZU coastal study sites for pre-fire (unburned), or baseline conditions (Figure 5). The CZU August Lightning Complex site, located in Santa Cruz county, displayed a 0.82 NDVI baseline value. Additionally, the Woodward site, located in Point Reyes, showed a baseline NDVI value of 0.76. These values were contrary to the initial hypothesis that the northernmost study site, Siskiyou, would have the highest baseline NDVI; Siskiyou had an NDVI baseline of 0.67.

However, coastal sites had higher NDVI values compared to more inland sites, which was an expected finding. For example, the Tubbs site, which is located in a more inland area in Sonoma County, had a baseline NDVI value of 0.65. The Kincade site, which is neighboring the Tubbs site in Sonoma County, also had a baseline NDVI of 0.62. The Walbridge study site, which is also relatively inland, experienced a baseline NDVI value of 0.73.

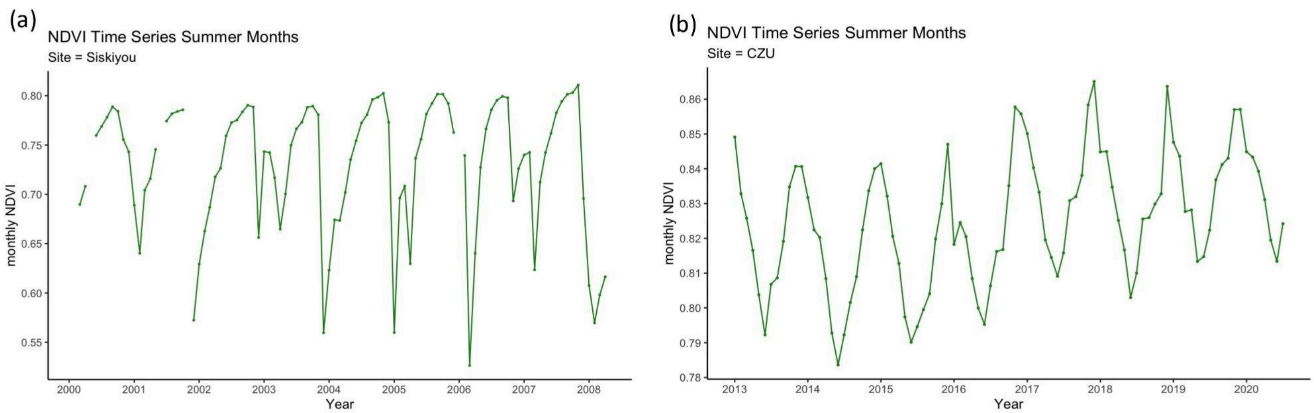

Figure 5. Average NDVI Time Series for summer months. (a) Siskiyou study site in the far north of California, (b) CZU August Lightning complex study site in the southern end of the study region, Santa Cruz county.

Another finding was the notable drop-off in NDVI for all study sites after a fire event. For example, the Walbridge fire in 2020 caused a decrease in NDVI by 0.25, and NDVI was still decreased by 0.16 two years later (Figure 6). The high severity coastal forest fires caused a significant drop off in NDVI.

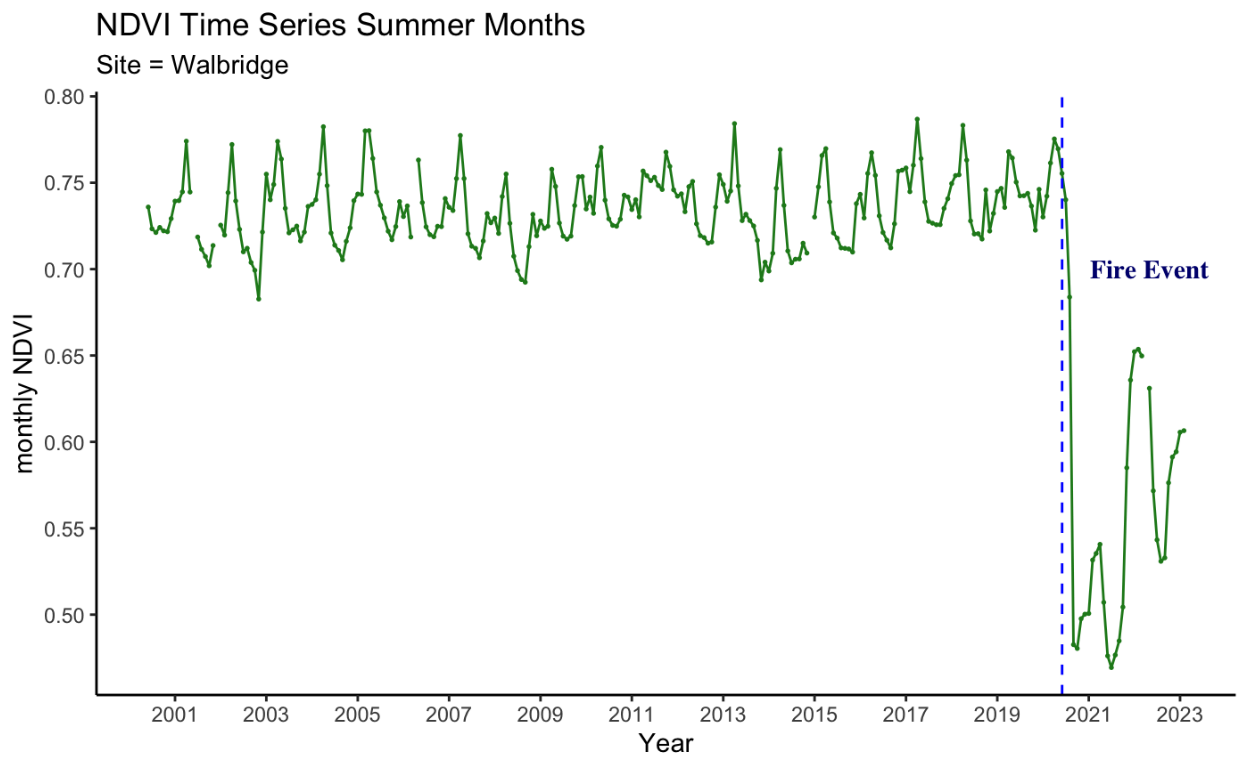

Figure 6. A monthly NDVI time series from the Walbridge study site. The site is located in western Sonoma County, and the time spans from 2000-2023, with the fire ignition event as a dashed line.

FLCC and NDVI Time Series

The FLCC proportion and average monthly NDVI were scaled for comparison for each site, and compared. One notable example is the Walbridge study site, where NDVI and FLCC track each other closely from 2000 until 2007, when they drastically diverged (Figure 7). During the period from 2007 to 2010, FLCC proportion levels are high, while NDVI experiences a decrease.

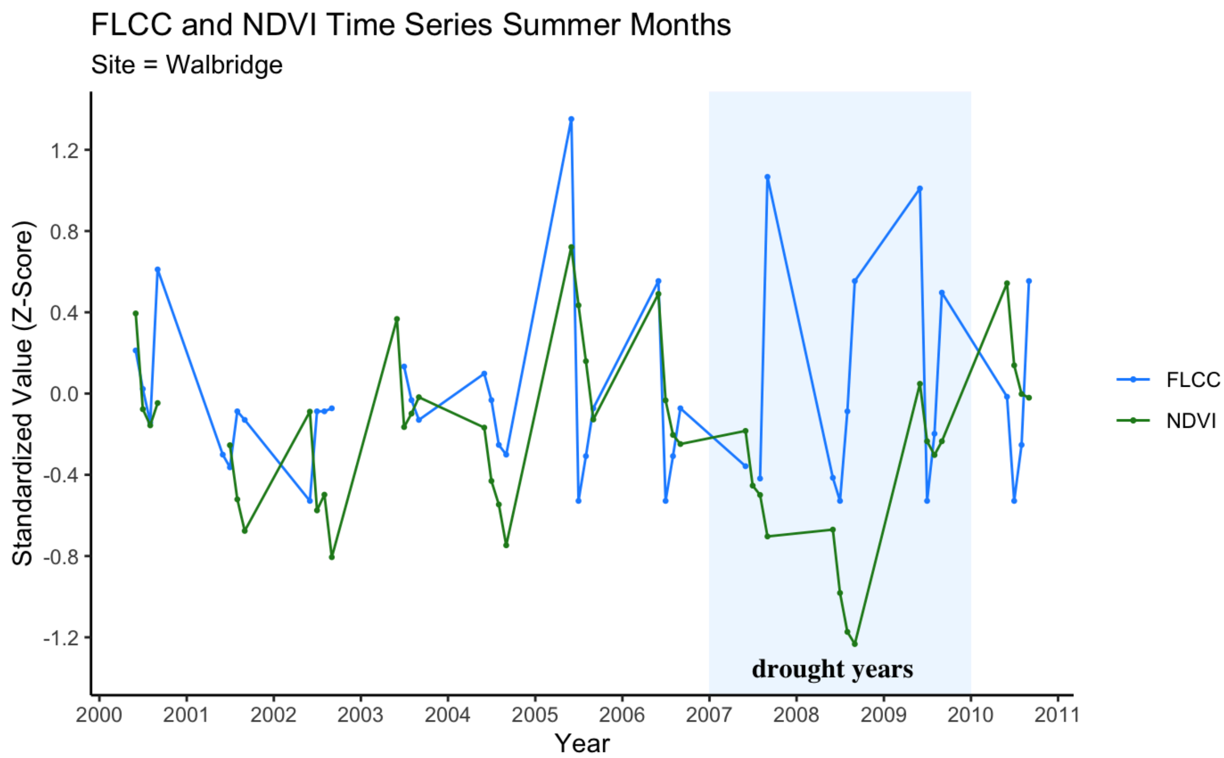

Figure 7. A time series of both monthly NDVI and FLCC in the Walbridge fire study site, zoomed into years 2000-2011. The drought period is highlighted, and the variables are scaled for direct comparison.

The coastal site of Woodward in Point Reyes experienced among the highest fog days per month, with up to 21 days of FLCC detection, while also displaying high levels of baseline NDVI of around 0.76. The Walbridge inland site experienced a lower level of FLCC, with a high of 8 days per month. The Siskiyou northern site had high levels of FLCC, with the maximum value of 25 days per month, along with a baseline NDVI level of 0.76.

Fog and Burn Severity: GAM

After implementing the GAM model, I found that precipitation, maximum VPD, and the Enhanced Vegetative Index (EVI) were significant variables in predicting dNBR in the model. Mean temperature and proportion of fog days were not significant in prediction power (Table 3). The statistic metric indicates that variables with a higher value have a more significant contribution to the model. Average EVI was exceptionally high at a 55.23 statistic value, and precipitation followed with 4.65, along with maximum VPD at a 3.00 statistic value.

Additionally, the edf (estimated degrees of freedom) metric suggests that variables with a higher edf value display a more flexible model fit, which allows for more curvature in the relationship between the predictor and the response variable. Precipitation had the most flexibility, with an edf of 9.68. Fog proportion and average temperature were the lowest, with an edf of 1.0. Variables with a significant p-value of ≤ 0.05 were precipitation, maximum VPD, and average EVI, while fog proportion and mean temperature did not meet this threshold.

Table 3. Results of burn severity GAM model. Columns include terms (average temperature, precipitation, maximum VPD, average EVI, and fog (FLCC) proportion), along with edf (estimated degrees of freedom), statistic, and p-value.

term <chr>	edf <dbl>	statistic <dbl>	p.value <dbl>
s(t_mean)	1.000000	0.1698501	0.68150
s(ppt)	8.679596	4.6551845	0.00010
s(vpd_max)	2.920492	3.0015594	0.02867
s(Avg_EVI)	4.519449	55.2338035	0.00000
s(fog_prop)	1.000000	1.2610827	0.26528

Furthermore, the model was responsible for 88.4% of deviance explained, along with a high adjusted R-squared value of 0.854 (Figure 8). The R-squared provides a measure of how well the variability in the response variable is explained by the model. Here, 85.4% of the variance in the response is explained by the predictors in the model, adjusted for the number of predictors. Additionally, the Generalized Cross-Validation score was 0.0042549. This metric is used to assess the model's predictive performance or tuning the model's smoothing parameters, and a lower value indicates a better model fit (Scheipl 2011). The estimated scale parameter used in the model, scale est., is related to the variance of the error terms. The small value, 0.0033409, indicates less error variance and therefore a better fit of the model to the data.

```
R-sq.(adj) =  0.854   Deviance explained = 88.4%
GCV = 0.0042549  Scale est. = 0.0033409  n = 89
```

Figure 8. Results of the burn severity GAM model. Outputs include R-squared, deviance explained, Generalized Cross Validation (GCV) score, and scale est. (scale parameter, estimated).

Fog Trends

After creating a time series of FLCC days per month, I found that FLCC fluctuates on a yearly basis with no clear increase or decrease over the study period for all sites. Examining the Wallbridge site as an example, there is a slight increase during the years 2011 to 2017, but no notable trends otherwise (Figure 9). For this site, there is high variation in the data, with fog days occurring as low as zero in one month, and up to eight days per month at other points.

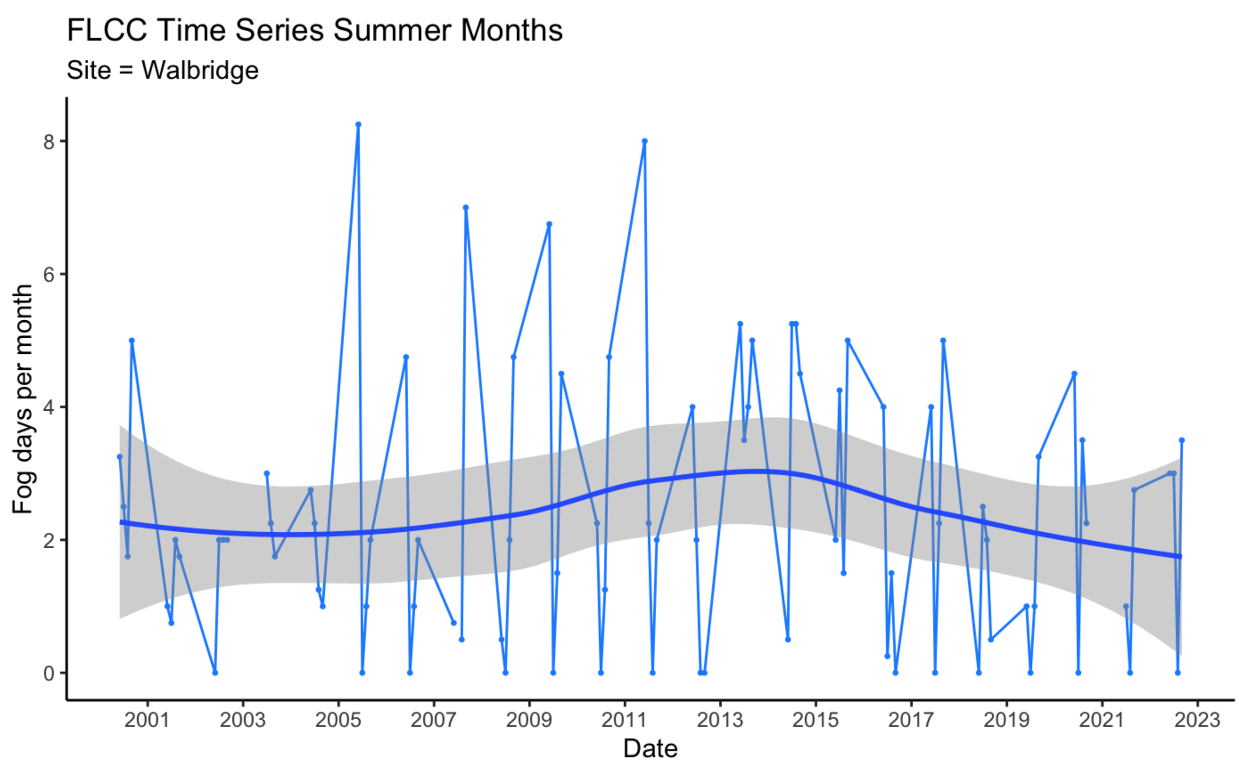

Figure 9. A time series of FLCC in the Walbridge fire study site from 2000-2022. Site in western Sonoma County.

Pre-fire Ignition Conditions

I found that for fire ignition conditions at each location, results were consistent across study sites. For example, at the Woodward study site in Point Reyes, FLCC proportion and precipitation, while high at the actual time of ignition, displayed lower values for the preceding year period (Figure 10). Additionally, mean temperature and maximum VPD values were both elevated at the time of fire ignition events. These conditions were similarly significant at all six study sites.

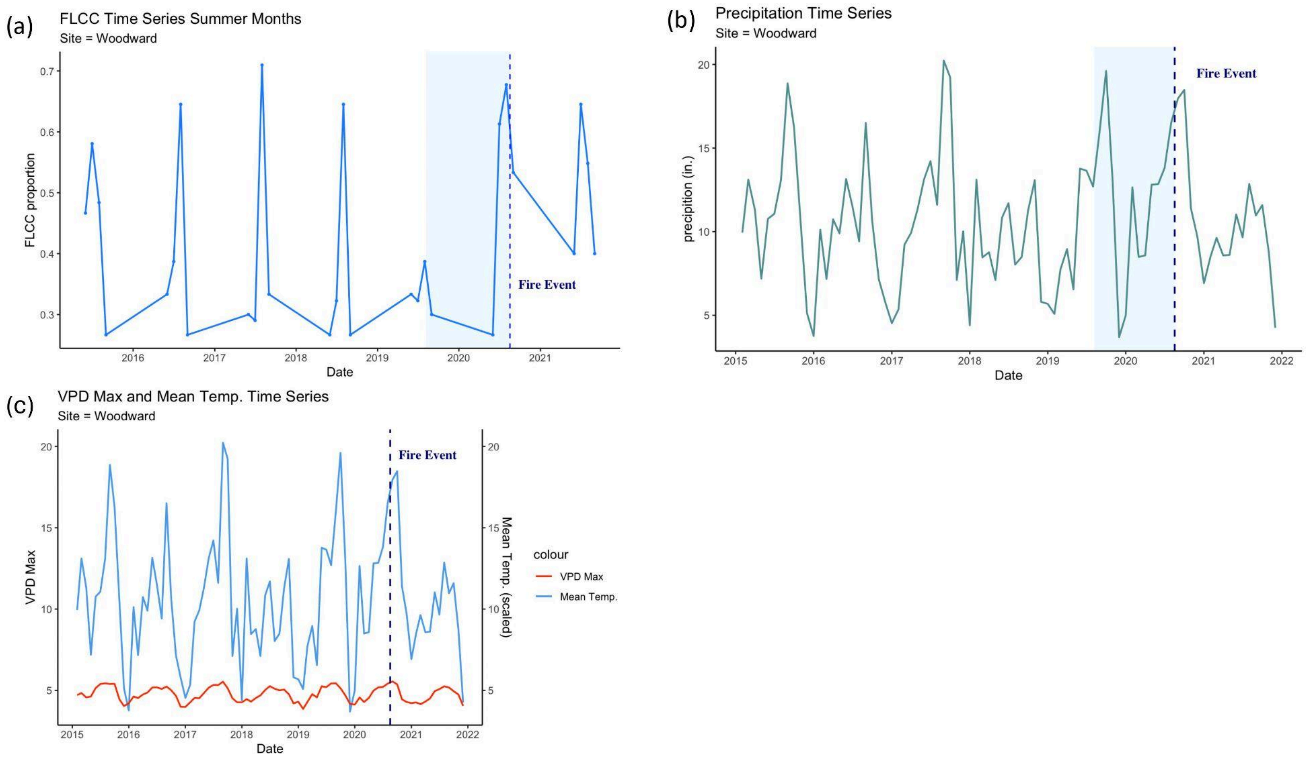

Figure 10. Time series of climatic variables for pre-fire period conditions, for the Woodward study site. (a) Fog and Low Cloud Cover (FLCC), with preceding one year highlighted, (b) precipitation, with preceding one year highlighted, (c) Vapor Pressure Deficit (VPD) maximum and mean temperature, with temp. scaled for comparison.

DISCUSSION

Fog Levels and Vegetation Growth Through NDVI

This study helped convey the ecological role and importance of fog in maintaining vegetation health. Findings highlight the dependency of vegetation on FLCC (Burgess 2004), especially during the arid summer months of the region's Mediterranean climate (Giorgi 2008). In coast redwood forests of northern California, the study by Dawson (1998) found that *S. sempervirens* receives 19% of its summer water from fog and fog drip. In examining the summer monthly NDVI and FLCC proportion for each study site, I found that contrary to my hypothesis, the northernmost site, Siskiyou, did not experience the highest levels of NDVI, despite having the highest FLCC occurrence of a maximum of 25 days per month. There are multiple possibilities for these NDVI values. The rapid drops in value from the NDVI time series for Siskiyou indicate likely sensor interference due to the high FLCC presence during the summer. A study by Motohka (2011) found that residual small clouds were attributed to contamination of about 40% of their MODIS data after cloud screening. These findings indicated that cloud interference significantly decreased NDVI values during the growing season. Noise due to clouds was found to be a severe problem for time series monitoring in another study by Salgado (2023), which used satellite sensors with low-to-medium spatial resolution such as the Terra and Aqua MODIS satellites. In my study, the NDVI dataset was a 16-day composite, but despite the averaging of NDVI across this period, I still found images that were missing pixels and had to filter them out. In the case of Siskiyou, sensor disruption seems likely, as fog presence is so high that even a cloud filter might not yield a time series free of noise.

Another finding of the study was the proximity to the coast as more important in indicating FLCC, rather than the latitudinal gradient of increased fog presence towards the Oregon border. Multiple studies have found that coastal fog tends to be denser and more persistent compared to inland areas due to onshore marine influences and specific microclimates along the coast (Weiss-Penzias 2012, Sawaske 2015, Baguskas 2016). These findings explain why coastal sites such as Woodward and CZU had higher FLCC and NDVI values compared to more inland sites like Tubbs, Kincade, and Walbridge. Additionally, the Tubbs and Kincade sites included urban development, which also contributes to a lower NDVI average value (Lee 2023), as predominantly built environment materials will reflect lower greenness overall.

I also found strong linear patterns between FLCC proportion and average summer NDVI for each study site, with exceptions during drought periods. While the scatterplot of the two variables did not reveal any linear trends, comparing the scaled values revealed a strong relationship. A study by Ball (2020) had similar findings, with fog distributions correlating with patterns of vegetation greenness, and an overall increase in greenness with fog density. In considering drought, many studies have been able to discover a sharp decline in NDVI values during drought periods (Rousta 2020, Ding 2022, Wang 2023). A study by Corbin (2005) found that 28-66%, depending on species, of the water taken up by plants via roots during summer drought came from fog rather than winter rain. However, these summer fog inputs are often not sufficient during years of abnormally low winter rain, leading to lower NDVI values despite higher FLCC presence during drought conditions.

Fog Occurrence During Fire Season and Wildfire Severity

The results of the GAM model showed that precipitation, maximum VPD, and average EVI were significant, while fog proportion and mean temperature did not meet this threshold. While temperature on its own is not significant in this case, temperature is incorporated into the VPD calculation (Holden 2018). Therefore, maximum VPD is a strong variable in dNBR prediction power. Fog proportion was not a significant variable in the model, which suggests not only do the limitations of the FLCC dataset need to be considered, but also that other methodologies should be considered in creating the burn severity model. Pre-fire conditions were more informative; heightened maximum VPD values at ignition events were in-line with findings from studies by Sedano (2014) and Seager (2015). Sedano found a significant relationship between daily VPD and the probability that a lightning strike would develop into a fire. Additionally, they found that above average VPD following ignition increased the likelihood that fires would grow to be significantly large. A study by Michelle (2021) verified that VPD is an essential climate indicator for forest fires, as it represents the stress conditions for vegetation prone to fires. While not significant in the model, FLCC still plays an important role in coastal forests through its effects on lowering temperatures and increasing moisture levels (Torregrosa 2016), acting as an ecosystem component that helps moderate fire behavior.

Overall Fog Patterns and Implications

Contrary to my hypothesis, fog patterns over the course of the study period, from 2000 to 2022, did not experience a significant decreasing trend. This result suggests a high level of variability in fog occurrence, which reflects the complex interplay of local and regional climatic factors driving fog formation (Koračin 2014). These findings are also at odds with results from Johnstone (2010), which was able to extrapolate a ~33% decrease in fog hours since the early 20th century. There are multiple possibilities for this discrepancy. The Johnstone study has data until 2010, so my study examines an additional 12 years beyond this point. Interestingly, another study by Lebassi (2009) found a decreasing trend in coastal California summer daytime maximum temperatures since 1970, and suggested an increase in “cool sea-breeze flows and its associated coastal stratus”, or fog, as a primary cause. Additionally, there are some limitations of the FLCC dataset from MODIS. The study by Werner (2022) used the MODIS cirrus cloud flag, identifying clouds above 6 km, removing these, and then considering all remaining clouds as FLCC. This assumption is based on the study by Francis (2020), which says “low-level marine stratus clouds comprise more than 75% of clouds on the coast of California” during the summer months. Additionally, FLCC burn-off time is quite variable (Haeffelin 2010), and if it is not present during the MODIS 10:30 am overpass time, then FLCC presence for that day will not be recorded. The absence of a discernible long-term trend in fog occurrence highlights the challenges in predicting fog (Kim 2022) and anticipating the ecological impacts of changing trends, which underlines the need for continuous monitoring and advanced modeling techniques to better understand these dynamics.

Future Directions

Fog plays a multifaceted role in influencing vegetation health and wildfire dynamics in the Northern California coastal forests. The observed relationships between FLCC, vegetation growth, and burn severity demonstrate the importance of atmospheric climatic factors in terrestrial ecosystems. Furthermore, the discovered variability in fog patterns and their impacts calls for further research. Future studies should focus on refining remote sensing methodologies to capture more detailed fog dynamics and explore the interactions between fog, climate change, and ecosystem responses. For example, the refinement of satellite products, such as MODIS, and development of an improved cloud detection system can increase the validity of results for future applications. Additionally, incorporating longer temporal datasets and more sophisticated climate models could enhance understanding of how coastal ecosystems evolve under changing climate scenarios. Although NDVI is the most common spectral index for monitoring vegetation changes (Tucker 1979), the study results also indicate that noise from residual clouds is minimized when using other indices like EVI, NDWI, or NDII instead of NDVI. Future studies should integrate additional environmental variables, such as soil moisture levels or wind patterns, to further improve the predictive capabilities of wildfire models.

Broader Implications and Management

The broader implications of this study are highly relevant to ecosystem management, wildfire mitigation strategies, and climate adaptation efforts. By continuing to improve understanding of FLCC impacts on wildfire ignition, implications of fog dynamics will be better understood. As coastal forest ecosystems continue to face the challenges of climate change and increasing wildfire risks, it is crucial that research continues to evolve, enabling better preparedness and response strategies to protect these critical natural environments and the communities that depend on them. Understanding the fog-fire relationship inside coastal forests is a key aspect of ecosystem management in order to carry out informed wildfire preparedness and climate adaptation strategies. Creating a hazardous condition detection system using remote sensing tools would be highly impactful in creating warnings when wildfire ignitions are most likely to occur, helping to protect vulnerable groups that are at the highest risk of experiencing negative effects of high severity fires or other climate disasters.

ACKNOWLEDGEMENTS

This thesis would not have been possible without the help of professors, graduate students, friends, and family who supported me throughout this process. First, a tremendous thank you to my mentor, Professor Todd Dawson, whose expertise surrounding fog and coast redwoods helped shape this project into what it is today. I am so grateful you were as excited about my thesis topic as I was and took me under your wing. Another immense thank you to Minho Kim, my GIS professor and an incredible mentor figure for remote sensing topics, applying to grad school, and life advice, whose passion continues to inspire me to this day. Thank you to PhD student Marriane Cowherd, expert in wildland fire, for your kindness and willingness to help me with tackling tricky questions in my methodology, along with grad school apps. Another thank you to PhD student Annie Taylor, whose resourcefulness with Google Earth Engine has helped advance my thesis greatly. To Zack Werner, a creator of the MODIS Fog and Low Cloud Cover Application, thank you for sharing your data with me and being a great collaborator during this process. Additionally, thank you to Eric Waller from USGS, who gave me great insight about remote sensing and Google Earth Applications, along with USGS's Alicia Torregrosa, who is the reason that I discovered Zack's dataset in the first place. To Professor Dennis Baldocchi, thank you for your optimism and support of my thesis, along with imparting me with extensive ecosystem ecology knowledge. Thank you also to Professor Peter Weiss from UCSC for your fog expertise and insights, along with Dr. James Johnstone for your extensive work on fog, which has helped pave the way for my project. Thank you to Dr. Rachel Clemesha from the Scripps Institution for your remote sensing work on marine layer clouds. A huge thank you to the ESPM 175 Teaching Team, especially Professor Patina Mendez and Annie Miller; you saw this thesis grow from an idea to a full fledged project. Thank you to my friends from ES who supported me throughout this process: Priya Riley, Megan Hur (thank you for thesis party!), Jiawen Tang, Ethan Xie, Akshay Patel, Patrick Jacobson, Xiangrong (Mark) Sun, Isabel Martin, Zcjanin Ollesca, and more. And finally, thank you to my wonderful family: Jack, Akiko, and Saki Burns. I am incredibly fortunate to have so many people who supported me on my thesis journey.

REFERENCES

Abatzoglou, J. T., and C. A. Kolden. 2013. Relationships between climate and macroscale area burned in the western United States. International Journal of Wildland Fire 22:1003–1020.

Baguskas, S., C. Still, D. Fischer, C. D'Antonio, and J. King. 2016. Coastal fog during summer drought improves the water status of sapling trees more than adult trees in a California pine forest: Oecologia. Oecologia 181:137–148.

Ball, L., and J. Tzanopoulos. 2020. Interplay between topography, fog and vegetation in the central South Arabian mountains revealed using a novel Landsat fog detection technique. Remote Sensing in Ecology and Conservation 6:498–513.

Burgess, S. S. O., and T. E. Dawson. 2004. The contribution of fog to the water relations of Sequoia sempervirens (D. Don): foliar uptake and prevention of dehydration. Plant, Cel & Environment 27:1023–1034.

Cermak, J. 2018. Fog and Low Cloud Frequency and Properties from Active-Sensor Satellite Data. Remote Sensing 10:1209.

Chen, D., J. Norris, N. Goldenson, C. Thackeray, and A. Hall. 2021. A Distinct Atmospheric Mode for California Precipitation. Journal of Geophysical Research: Atmospheres

126:e2020JD034403.

Cooper, W. S. 1917. Redwoods, Rainfall and Fog. The Plant World 20:179–189.

Corbin, J. D., M. A. Thomsen, T. E. Dawson, and C. M. D'Antonio. 2005. Summer water use by California coastal prairie grasses: fog, drought, and community composition. Oecologia 145:511–521.

Dawson, T. E. 1998. Fog in the California redwood forest: ecosystem inputs and use by plants. Oecologia 117:476–485.

Delcourt, C. J. F., A. Combee, B. Izbicki, M. C. Mack, T. Maximov, R. Petrov, B. M. Rogers, R. C. Scholten, T. A. Shestakova, D. van Wees, and S. Veraverbeke. 2021. Evaluating the Differenced Normalized Burn Ratio for Assessing Fire Severity Using Sentinel-2 Imagery in Northeast Siberian Larch Forests. Remote Sensing 13:2311.

Dillon, G. K., Z. A. Holden, P. Morgan, M. A. Crimmins, E. K. Heyerdahl, and C. H. Luce. 2011. Both topography and climate affected forest and woodland burn severity in two regions of the western US, 1984 to 2006. Ecosphere 2:art130.

Ding, Y., X. He, Z. Zhou, J. Hu, H. Cai, X. Wang, L. Li, J. Xu, and H. Shi. 2022. Response of vegetation to drought and yield monitoring based on NDVI and SIF. CATENA 219:106328.

Eastman, J. R., F. Sangermano, E. A. Machado, J. Rogan, and A. Anyamba. 2013. Global Trends in Seasonality of Normalized Difference Vegetation Index (NDVI), 1982–2011. Remote Sensing 5:4799–4818.

Eisfelder, C., S. Asam, A. Hirner, P. Reiners, S. Holzwarth, M. Bachmann, U. Gessner, A. Dietz, J. Huth, F. Bachofer, and C. Kuenzer. 2023. Seasonal Vegetation Trends for Europe over 30 Years from a Novel Normalised Difference Vegetation Index (NDVI) Time-Series—The TIMELINE NDVI Product. Remote Sensing 15:3616.

Erard, C. 2017. Bonan, G.— Ecological climatology. Concepts and applications. Third edition. Cambridge University Press, Cambridge & New York, 2016.

Fensholt, R., and S. R. Proud. 2012. Evaluation of Earth Observation based global long term vegetation trends — Comparing GIMMS and MODIS global NDVI time series. Remote Sensing of Environment 119:131–147.

Fernández, M., H. H. Hamilton, and L. M. Kueppers. 2015. Back to the future: using historical climate variation to project near-term shifts in habitat suitable for coast redwood. Global Change Biology 21:4141–4152.

Filonczuk, M. K., D. R. Cayan, and L. G. Riddle. 1995. Variability of marine fog along the California coast

Francis, E. J., G. P. Asner, K. J. Mach, and C. B. Field. 2020. Landscape scale variation in the hydrologic niche of California coast redwood. Ecography 43:1305–1315.

Funk, C. C., and M. E. Brown. 2006. Intra-seasonal NDVI change projections in semi-arid Africa. Remote Sensing of Environment 101:249–256.

Giorgi, F., and P. Lionello. 2008. Climate change projections for the Mediterranean region. Global and Planetary Change 63:90–104.

Grünig, M., R. Seidl, and C. Senf. 2023. Increasing aridity causes larger and more severe forest fires across Europe. Global Change Biology 29:1648–1659.

Gultepe, I., G. Pearson, J. A. Milbrandt, B. Hansen, S. Platnick, P. Taylor, M. Gordon, J. P. Oakley, and S. G. Cober. 2009. The Fog Remote Sensing and Modeling Field Project. Bulletin of the American Meteorological Society 90:341–360.

Haeffelin, M., T. Bergot, T. Elias, R. Tardif, D. Carrer, P. Chazette, M. Colomb, P. Drobinski, E. Dupont, J.-C. Dupont, L. Gomes, L. Musson-Genon, C. Pietras, A. Plana-Fattori, A. Protat, J. Rangognio, J.-C. Raut, S. Rémy, D. Richard, J. Sciare, and X. Zhang. 2010. PARISFOG: Shedding New Light on Fog Physical Processes. Bulletin of the American Meteorological Society 91:767-773,775-783.

Halofsky, J. E., D. L. Peterson, and B. J. Harvey. 2020. Changing wildfire, changing forests: the effects of climate change on fire regimes and vegetation in the Pacific Northwest, USA. Fire Ecology 16:4.

Holden, Z. A., A. Swanson, C. H. Luce, W. M. Jolly, M. Maneta, J. W. Oyler, D. A. Warren, R. Parsons, and D. Affleck. 2018. Decreasing fire season precipitation increased recent western US forest wildfire activity. Proceedings of the National Academy of Sciences of the United States of America 115:E8349–E8357.

Huang, Y., Y. Jin, M. W. Schwartz, and J. H. Thorne. 2020. Intensified burn severity in California's northern coastal mountains by drier climatic condition. Environmental Research Letters 15:104033.

Huntington, J. L., K. C. Hegewisch, B. Daudert, C. G. Morton, J. T. Abatzoglou, D. J. McEvoy, and T. Erickson. 2017. CLIMATE ENGINE: Cloud Computing and Visualization of Climate and Remote Sensing Data for Advanced Natural Resource Monitoring and Process Understanding. Bulletin of the American Meteorological Society 98:2397–2409.

Iacobellis, S. F., and D. R. Cayan. 2013. The variability of California summertime marine stratus: Impacts on surface air temperatures. Journal of Geophysical Research: Atmospheres 118:9105–9122.

Jensen, M. P., A. M. Vogelmann, W. D. Collins, G. J. Zhang, and E. P. Luke. 2008. Investigation of Regional and Seasonal Variations in Marine Boundary Layer Cloud Properties from MODIS Observations. Journal of Climate 21:4955–4973.

Jiang, Z., A. R. Huete, K. Didan, and T. Miura. 2008. Development of a two-band enhanced vegetation index without a blue band. Remote Sensing of Environment 112:3833–3845.

Johnstone, J. A., and T. E. Dawson. 2010. Climatic context and ecological implications of summer fog decline in the coast redwood region. Proceedings of the National Academy of Sciences 107:4533–4538.

Johnstone, J. A., J. S. Roden, and T. E. Dawson. 2013. Oxygen and carbon stable isotopes in coast redwood tree rings respond to spring and summer climate signals. Journal of Geophysical Research: Biogeosciences 118:1438–1450.

Kim, S., C. Rickard, J. Hernandez-Vazquez, and D. Fernandez. 2022. Early Night Fog Prediction Using Liquid Water Content Measurement in the Monterey Bay Area. Atmosphere 13:1332.

Koračin, D., C. E. Dorman, J. M. Lewis, J. G. Hudson, E. M. Wilcox, and A. Torregrosa. 2014. Marine fog: A review. Atmospheric Research 143:142–175.

Lebassi, B., J. González, D. Fabris, E. Maurer, N. Miller, C. Milesi, P. Switzer, and R. Bornstein. 2009. Observed 1970–2005 Cooling of Summer Daytime Temperatures in Coastal California. Journal of Climate 22:3558–3573.

Lee, G. 2022. Vegetation Classification in Urban Areas by Combining UAV-Based NDVI and Thermal Infrared Image. https://www.mdpi.com/2076-3417/13/1/515.

Mahdizadeh, M. 2021. Initial Floristic Response to High Severity Wildfire in an Old-Growth Coast Redwood (Sequoia sempervirens (D. Don) Endl.) Forest. Forests 12:1135.

Matci, D., and U. Avdan. 2020. Comparative analysis of unsupervised classification methods for mapping burned forest areas. Arabian Journal of Geosciences 13:711

Michelle, F., C. Dominguez, A. Espinoza, A. Jaramillo, A. Camilo, V. Maldonado, I. Tovar, and F. Alejandro. 2021. Forest fire probability under ENSO conditions in a semi-arid region: a case study in Guanajuato. Environmental Monitoring and Assessment 193.

Miller, J. D., H. D. Safford, M. Crimmins, and A. E. Thode. 2009. Quantitative Evidence for Increasing Forest Fire Severity in the Sierra Nevada and Southern Cascade Mountains, California and Nevada, USA. Ecosystems 12:16–32.

Motohka, T., K. N. Nasahara, K. Murakami, and S. Nagai. 2011. Evaluation of Sub-Pixel Cloud Noises on MODIS Daily Spectral Indices Based on in situ Measurements. Remote Sensing 3:1644–1662.

Nghiem, J., C. Potter, and R. Baiman. 2019. Detection of Vegetation Cover Change in Renewable Energy Development Zones of Southern California Using MODIS NDVI Time Series Analysis, 2000 to 2018. Environments 6:40.

Noss, R. F., Save-the-Redwoods League. 2013. The Redwood Forest: History, Ecology, and Conservation of the Coast Redwoods. Island Press, Chicago, UNITED STATES.

Petreshen, J. 2021. Fog Presence and Ecosystem Responses in a Managed Coast Redwood Forest.

Pettorelli, N., J. O. Vik, A. Mysterud, J.-M. Gaillard, C. J. Tucker, and N. Chr. Stenseth. 2005. Using the satellite-derived NDVI to assess ecological responses to environmental change. Trends in Ecology & Evolution 20:503–510.

Potter, C. 2016. Thirty years of vegetation change in the coastal Santa Cruz Mountains of Northern California detected using landsat satellite image analysis. Journal of Coastal Conservation 20:51–59.

Potter, C. 2023, April 12. Impacts of the CZU Lightning Complex Fire of August 2020 on the forests of Big Basin Redwoods State Park. https://journal.wildlife.ca.gov/2023/04/12/impacts-of-the-czu-lightning-complex-fire-of-august-2020-on-the-forests-of-big-basin-redwoods-state-park/.

Rao, K., A. P. Williams, N. S. Diffenbaugh, M. Yebra, C. Bryant, and A. G. Konings. 2023. Dry Live Fuels Increase the Likelihood of Lightning-Caused Fires. Geophysical Research Letters 50:e2022GL100975.

Rousta, I., Ólafsson, H. 2020. Impacts of Drought on Vegetation Assessed by Vegetation Indices and Meteorological Factors in Afghanistan. Remote Sensing 12:2433.

Salgado, C. B., O. A. de Carvalho Júnior, R. A. T. Gomes, and R. F. Guimarães. 2023. Cloud interference analysis in the classification of MODIS-NDVI temporal series in the Amazon region, municipality of Capixaba, Acre - Brazil. Sociedade & Natureza 31:e47062.

Sawaske, S. R., and D. L. Freyberg. 2015. Fog, fog drip, and streamflow in the Santa Cruz Mountains of the California Coast Range: Ecohydrology. Ecohydrology 8:695–713.

Scheipl, F. 2011. spikeSlabGAM: Bayesian Variable Selection, Model Choice and Regularization for Generalized Additive Mixed Models in R. Journal of Statistical Software 43:1–24.

Seager, R., A. Hooks, A. P. Williams, B. Cook, J. Nakamura, and N. Henderson. 2015. Climatology, Variability, and Trends in the U.S. Vapor Pressure Deficit, an Important Fire-Related Meteorological Quantity. Journal of Applied Meteorology and Climatology 54:1121–1141.

Sedano, F., and J. T. Randerson. 2014. Multi-scale influence of vapor pressure deficit on fire ignition and spread in boreal forest ecosystems: Biogeosciences. Biogeosciences 11:3739–3755.

Sidhu, N., E. Pebesma, and G. Câmara. 2018. Using Google Earth Engine to detect land cover change: Singapore as a use case. European Journal of Remote Sensing 51:486–500.

Stasinopoulos, M. D., T. Kneib, N. Klein, A. Mayr, and G. Z. Heller. 2024. Generalized Additive Models for Location, Scale and Shape: A Distributional Regression Approach, with Applications. Cambridge University Press, Cambridge.

Subhanil, G., and G. Himanshu. 2022. Seasonal variability of LST-NDVI correlation on different land use/land cover using Landsat satellite sensor: a case study of Raipur City, India. Environment, Development and Sustainability 24:8823–8839.

Torregrosa, A., T. A. O'brien, and I. C. Faloona. 2014. Coastal fog, climate change, and the environment. Eos 95:473–474.

Torregrosa, A., C. Combs, and J. Peters. 2016. GOES-derived fog and low cloud indices for coastal north and central California ecological analyses, Earth and Space Science, 3, doi:10.1002/2015EA000119.

Tucker, C. J. 1979. Red and photographic infrared linear combinations for monitoring vegetation. Remote Sensing of Environment 8:127–150.

U.S. Geological Survey. 2022. Rapid Assessment of Vegetation after Wildfire (RAVG) Interactive Viewer. https://burnseverity.cr.usgs.gov/viewer/?product=RAVG.

van Mantgem, P. J., J. C. B. Nesmith, M. Keifer, E. E. Knapp, A. Flint, and L. Flint. 2013. Climatic stress increases forest fire severity across the western United States. Ecology Letters 16:1151–1156.

Waller, E. K. 2014. Complexity in Climatic Controls on Plant Species Distribution: Satellite Data Reveal Unique Climate for Giant Sequoia in the California Sierra Nevada. UC Berkeley.

Wang, Y., and J. Song. 2023. Field-Measured Hydraulic Traits and Remotely Sensed NDVI of Four Subtropical Tree Species Showed Transient Declines during the Drought–Heatwave Event. Forests 14:1420.

Wasserman, T. N., and S. E. Mueller. 2023. Climate influences on future fire severity: a synthesis of climate-fire interactions and impacts on fire regimes, high-severity fire, and forests in the western United States. Fire Ecology 19:43.

Weathers, K., Ponette-Gonzalez A., Dawson, T. 2020. Medium, Vector, and Connector: Fog and the Maintenance of Ecosystems - ProQuest. https://www.proquest.com/docview/2220515594?pq-origsite=primo&sourcetype=Scholar

ly%20Journals.

Weiss-Penzias, P. S., C. Ortiz Jr., R. P. Acosta, W. Heim, J. P. Ryan, D. Fernandez, J. L. Collett Jr., and A. R. Flegal. 2012. Total and monomethyl mercury in fog water from the central California coast. Geophysical Research Letters 39.

Werner, Z., C. T. Hin Choi, A. Winter, A. G. Vorster, A. Berger, K. O'Shea, P. Evangelista, and B. Woodward. 2022. MODIS sensors can monitor spatiotemporal trends in fog and low cloud cover at 1 km spatial resolution along the U.S. Pacific Coast. Remote Sensing Applications: Society and Environment 28:100832.

Williams, A. P., R. Seager, A. K. Macalady, M. Berkelhammer, M. A. Crimmins, T. W. Swetnam, A. T. Trugman, N. Buenning, D. Noone, N. G. McDowell, N. Hryniw, C. I. Mora, and T. Rahn. 2014. Correlations between components of the water balance and burned area reveal new insights for predicting forest fire area in the southwest United States. International Journal of Wildland Fire 24:14–

Wood, S. 2017. Generalized Additive Models: An Introduction with R, 2 edition. Chapman and Hall/CRC.